AMERICAN SCIENTIFIC PUBLISHERS
Copyright © 2016 by American Scientific Publishers
All rights reserved.
Printed in the United States of America

Journal of
Nanoelectronics and Optoelectronics
Vol. 11, pp. 477–483, 2016
www.aspbs.com/jno

ARTICLE

Structure and Impedance Properties of Some Basalt Materials Under Magnetic Field

Meltem Çınar[1], Mehmet Kılıç[1], Yaşar Karabul[1], Nimet Yilmaz Canli[1], Ümit Alkan[2], Mustafa Okutan[1], and Orhan İçelli[1,*]

Volcanic basalt rocks are collected from different chemical compound, that is dark colored and comparatively rich in iron and magnesium, which is located at almost every country in the world. This study examined two different basalt samples collected from different regions of Van province in Turkey. The dielectric dispersion properties of the some Basalt rocks coded Sample 1 and Sample 2 were analyzed in order to determine the parameters such as surface conductivity, dissipation factor and complex dielectric functions. Morphological analysis, particle size measurement and electrical impedance analyzer measurements were assessed in order to determine dielectric constant, dielectric loss, dielectric strength and relaxation time. The research has revealed that due to its high dielectric dissipation and factor high resistance, Sample 1 can be used a precious material in numerous industrial applications that involve electromagnetic shielding or electrostatic dissipation applications.

Keywords: Basalt, Dielectric Constant, Dielectric Permittivity, Dielectric Loss, Magnetic Field.

1. INTRODUCTION

Basalt is a very widespread volcanic rock that is dark colored and relatively rich in iron and magnesium, almost located every country in the world. Basalt rocks include a variety of crucial elements (Fe, Mg, Ca, K, P, and S) along with helpful elements (Si and Na) for plants. Also, they are intrinsically obtainable and environmentally sound as a soil amendment.[1,2] Basalt is used for a wide variety of purposes: these rocks have been used in the refused rock industry, building tiles, construction industrial, highway engineering. Powders and fibers of basalt rocks are widely used of radiation shielding, thermal stability, heat and sound insulation.[3–7] In this study, basalt samples occurred in volcanic fields that were erupted from extensional fractures in a various durations in the Pliocene to Quaternary.[8,9]

The electrical characterization of samples is usually described by three essential electronic parameters: electrical conductivity, dielectric constant, and strength. Impedance spectroscopy measurements carried out on rocks have a superb significance because of the chance of correlating the microstructure of the system and the dielectric properties.[10,11] Dielectric researches are essential to comprehend the origin and the nature of dielectric losses, which, in turn, might be helpful in the determination of structure and defects in basalt rocks.[12] The electrical conductivity of matter and their variations are relatively well studied. The dielectric properties of rocks behave differently in terms of temperature and frequency, and have been studied.[13–16] But, there does not exist any report about dielectric properties of basalt samples under magnetic field. In particular, this issue has been studied for the first time in the magnetic field.

The aim of this work was to examine the electrical characteristic under magnetic field, especially on two types of basalt rocks. The samples were named as Sample 1 and Sample 2, respectively. Chemical composition, mineralogical assembles and textures of the rocks are studied in the different areas. Therefore, two different samples that represent the different volcanic region were obtained as well as classified in accordance with the chemical compositions.[9]

2. EXPERIMENTAL DETAILS

2.1. Materials

Chemical analyses of the basalt samples are taken by X-ray fluorescence (XRF) instrument. Operating

[1]Department of Physics, Faculty of Science and Letters, Yıldız Technical University, Istanbul, Turkey
[2]Department of Computer Engineering, Istanbul Gelişim University, Istanbul, Turkey
*Author to whom correspondence should be addressed.
Email: oicelli@yildiz.edu.tr
Received: 30.09.2015
Accepted: 20.11.2015

Table I. Chemical composition of basalt samples.

Compound	Sample 1	Sample 2
SiO_2	41.668	47.790
TiO_2	2.0800	1.3950
Al_2O_3	13.106	16.918
Fe_2O_3	13.823	10.878
MnO	0.1920	0.1630
MgO	9.7540	7.6190
CaO	10.602	11.357
Na_2O	5.2610	3.1370
K_2O	1.7370	0.5190
P_2O_5	1.7770	0.2240
Total	100.00	100.00

conditions of the Philips PW-2400 XRF instrument were set at 60 kV and 50 mA. The particle size and circularity measurements were taken with Malvern Mastersizer Hydro 200MU and micrograph photo taken by Malvern Morphology G3. X-ray diffraction measurements of basalt samples were taken using Rigaku Ultimo X-ray diffractometer with $Cu_{K\alpha}$ radiation, which has a wavelength about 1.5406 Å at a scan rate of 0.01°/s. The accelerating voltage was 40 kV and applied current was 30 mA. XRD patterns were studied in powdered basalt samples. Firstly, each one basalt type was homogenized with sieves 200 mesh. In order to prepare the pellet form, 1.8 g sieved basalt were added to 0.15 g cellulose. Each one of these mixtures prepared as a pellet having 13 mm diameter, 0.600 g weight and 2 mm thickness.

The results of chemical analysis of basalt samples are given in Table I. According to the chemical analysis of basalt samples, SiO_2 has pure basic character.

2.2. Particle Properties

Mastersizer device MS2000 carries out the classification processing of powder material in a wide measurement range of 0.02–2000 μm, and $\pm 1\%$ accuracy.

2.3. Morphology Analysis

Data with particle size, number and configuration (volume, diameter, length, etc.) are determined using Morphology analysis.

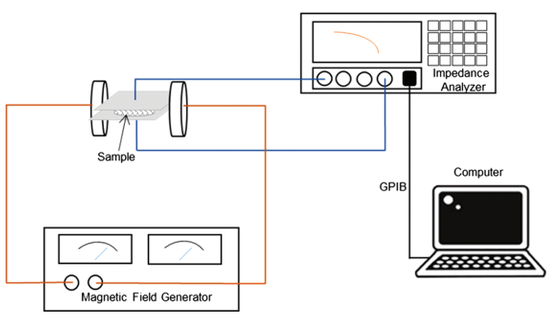


Fig. 1. The experimental set-up for dielectric measurements under magnetic field.

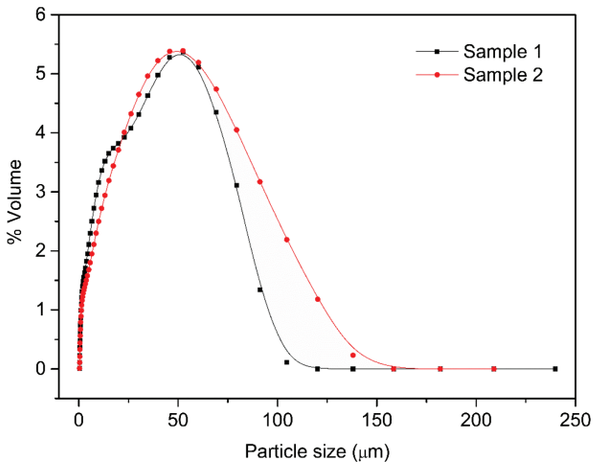


Fig. 2. Particle size of basalt samples.

2.4. Spectroscopy Analysis

Fourier-transform infrared spectroscopy analysis (FTIR) was performed on a Perkin Elmer Spectrum 400 one FTIR spectrometer. All spectra of basalt samples were taken in the 4000–650 cm^{-1} range, with a resolution of 2 cm^{-1} after 4 scans; the measurement was performed in the transmittance mode.

2.5. Thermal Analysis

TG/DTA is used to determine thermal gravimetric changes resulting in the structure of organic or inorganic samples as depending increasing the temperature or time. Thermo Gravimetry (TG) has examined changes such as water loss in order to remove organic matter. Temperature changes with exothermic or endothermic reaction occurring is determined by a Differential Thermal Analysis (DTA). The thermogravimetric analyses of Basalt rocks were performed on a Perkin-Elmer Pyris Diamond thermogravimetric-dynamic temperature analyzer

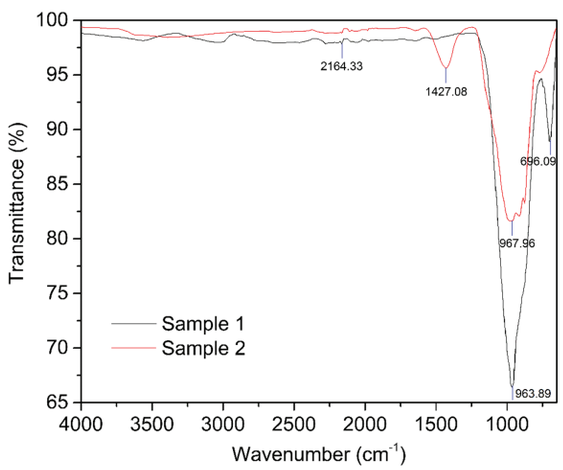


Fig. 3. FTIR of basalt samples.

Table II. TG/DTA of basaltic samples.

Sample	Melting temp. (°C)	Sample	Melting temp. (°C)	Sample	Melting temp. (°C)	Sample	Melting temp. (°C)
SiO_2	1600	Sc	154	Ba	727.0	Tm	1545
TiO_2	1843	V	1910	Cs	28.44	Yb	818.8
Al_2O_3	2072	Th	1755	La	920.0	Lu	1663
$Fe_2O_3^{TOT}$	1566	Co	1495	Ce	795.0	Hf	2231
MnO	1945	Ni	1455	Pr	930.8	Ta	3020
MgO	2852	Cu	1085	Nd	1021	Pb	327.5
CaO	2613	Zn	419.5	Sm	1074	U	1132
Na_2O	1132	Ga	29.77	Eu	826.0	W	3422
K_2O	350.0	Rb	39.48	Gd	1312	Sn	231.9
P_2O_5	340.0	Sr	768.8	Tb	1356	Mo	2623
TOT/C	–	Y	1522	Dy	1412	As	816.8
TOT/S	–	Zr	1855	Ho	1461		
LOI	–	Nb	2469	Er	1529		

(TG-DTA) with programmed heating at 10 °C/min from 30 °C to 700 °C.

2.6. Impedance Measurements

Impedance analyzers help us learn about the complex impedance of a system under test and electrical parameters such as dielectric constant and conductivity as frequency dependent. Impedance Spectroscopy (IS) has a powerful technique for characterizing the electrical properties of the basalt samples and their interfaces with electronically conducting electrodes.

The dielectric measurements were carried out with a two-point probe arrangement. The dielectric properties of the samples were measured on HP 4194A Impedance Analyzer under magnetic field (0–0.4 Tesla), in the room temperature at several frequencies from 100 Hz to 15 MHz. The experimental set-up for the measurements has been shown in Figure 1.

3. RESULTS AND DISCUSSION

The mastersizer values of basalt samples are given in Figure 2. 90 percent of the particles in Sample 1 and 2 have diameters of 0.972 and 0.968 μm respectively.

Performed FTIR analysis is given in the range of 650–4000 cm^{-1} in Figure 3. As seen in Figure 3, Sample 1 has a content of $ZrSiO_4$, Nb_2O_5, $SrTiO_3$, SiO, Al_2O_3, Fe_2O_3, MgO, CaO, Na_2O, K_2O, TiO_2, P_2O_5 and MnO. In evaluated analysis of FTIR of Sample 1, according to literature, 2164.33 cm^{-1} peak corresponds to Mg–C bond, 963.89 cm^{-1} peak corresponds to Cu–CO bond, and 696.09 cm^{-1} peak seen in the transmission spectrum of xCu_2O–$(100-x)MoO_3$. As seen in Figure 3, Sample 2 has a content of $BaMoO_4$, Co_3O_4, Nb_2O_5, Mg, Si, Fe, SiO_4. In evaluated analysis of FTIR of Sample 2, according to literature 1427.08 cm^{-1} peak corresponds to $SrTiO_3$, 967.96 cm^{-1} peak corresponds to Si–O bond. As a result, in FT-IR spectrum evaluated, Basalt samples have component such as SiO, Al_2O_3, Fe_2O_3, MgO, CaO, Na_2O, K_2O, TiO_2, P_2O_5, MnO, As and Ba.

The melting temperature of materials included in basalt samples is given in Table II. TG-DTA measurements is a range of 20–1000 °C. As seen in Figure 4, in the analysis of TG-DTA of 8.075 mg Sample 1, mass loss occurred depending on the temperature in the range of 33–625 °C. The mass loss of the sample occurred as 0.6% in the range of 33–670 °C. In the range of 670–1000 °C, an increase occurred in the mass of a sample resulting from the oxidation of the sample mass as the amount 0.2%. The exothermic reaction occurred during the measurement.

In evaluated analysis of TG-DTA of 7.378 mg Sample 2, in the range of 24 to 170 °C in the sample mass loss occurred as 0.7% depending on the temperature. In the range of 584–750 °C in the sample mass loss occurred as 2.2% depending on the temperature. The mass loss has not occurred in the range of 170–415 °C, almost. In this temperature range, samples take the heat. In the range of 810–815 °C in the sample mass loss occurred as 0.2% depending on the temperature. The sample mass loss did not occur in the range of 750–810 °C and 815–978 °C respectively. The exothermic reaction occurred during the measurement.

Morphology analysis values of basalt samples are presented in term of average diameter, length and volume analysis at Table III. When the measurements are

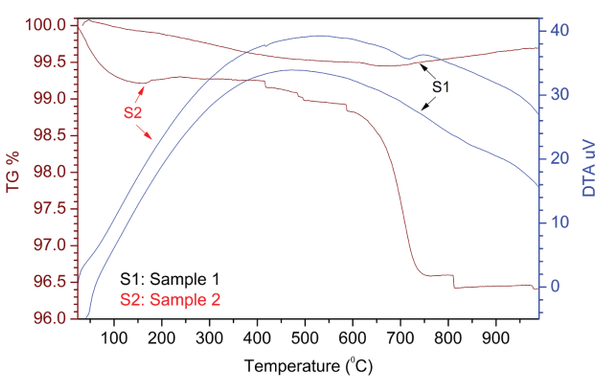


Fig. 4. TG-DTA of basalt samples.

Table III. Morphology analysis values of basalt samples.

Basalt Samples	Average diameter (μm)	90%, the particles have the diameter value	Average length (μm)	90%, the particles have the length value	Average volume (μm^3)	90%, the particles have the volume value
Sample 1	0.882	0.972	16.71	33.24	8153	6354
Sample 2	0.870	0.968	13.33	26.14	4121	2926

considered, the smallest value has been obtained from Sample 2 in terms of particle size, and circularity (in Table III).

Impedance analysis results; the state of the polarization in a material can be expressed by the dielectric constant. The degree of polarization of a material depends on density of dipoles oriented by the effect of external electric field. In this study, it is seen that decreases with increasing frequency of the dielectric constant of basalt samples. The reason for this decrease is attributed to polarization. The polarization has occurred with increasing frequency because it increases the effect of the dipole. Polarization is mainly due to electron exchange between Fe^{+2} and Fe^{+3} in the direction of applied magnetic field. A decrease in dielectric permittivity remains constant after the value of a particular frequency.

As seen in Figure 1, we examined the interaction with the magnetic field of materials in the experimental setup. The change in dielectric constant of basalt samples is plotted under magnetic field 0.1 T (1000 G) in Figure 5. As seen in Figure 5, when there is a significant interference in Sample 1 and Sample 2. The reason why such a situation occurs, attributed to the proportion of the magnetic element in the content of the sample. In low frequency, the dielectric constant of Sample 1 is higher than Sample 2. Furthermore, the constant of both have decreased in low frequency by magnetic field that affect the dielectric constant about 20% and 15% respectively. It is expected that the dielectric structure of ferromagnetic is made up of a conductive layer that consists of large ferrite grains. In Figure 6 examined, it is seen that the magnetic field does not affect dissipation factor (ε'').

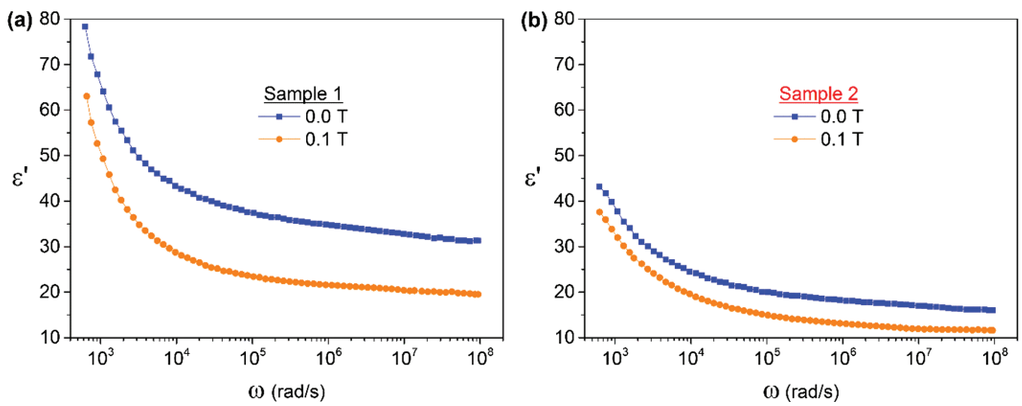


Fig. 5. The frequency-dependent change of dielectric constant in the magnetic field of (a) Sample 1 and (b) Sample 2.

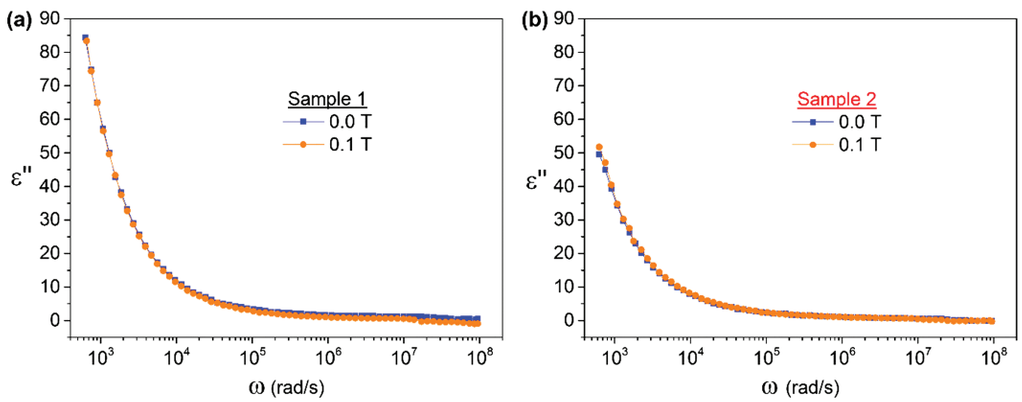


Fig. 6. Angular frequency-dependent variation of the imaginary part of dielectric constant depending magnetic field of (a) Sample 1 and (b) Sample 2.

Table IV. Dielectric strength parameters of the basalt samples under magnetic field.

	Sample 1			Sample 2		
B (Tesla)	ε'_s	ε'_∞	$\Delta\varepsilon'$	ε'_s	ε'_∞	$\Delta\varepsilon'$
0	78.38	31.28	47.10	43.22	16.09	27.13
0.1	63.02	19.55	43.47	37.58	11.59	25.99
0.2	63.02	19.61	43.41	40.68	14.66	26.02
0.3	62.97	19.63	43.34	41.04	15.13	25.91
0.4	62.53	19.66	42.87	40.62	14.99	25.63

The energy absorption ability of Sample 2 has higher than Sample 1 due to the fact that, the energy loss of Sample 2 is lower than another.

The values of the dielectric constant of the basalt samples are presented in Table IV. Using the values in this Table and $\Delta\varepsilon' = \varepsilon'_s - \varepsilon'_\infty$ equation, calculating dielectric strength values were plotted in Figure 7. As we have seen in this graph, Sample 1 and Sample 2 have high and low dielectric strength, respectively. Dielectric strength is weakened with the increasing magnetic field. Sample 1 is magnetic field interaction highest material. This state may be attributed to Fe_2O_3 content is %13.823 that is higher than others.

Changes with the magnetic field of the relaxation time (τ) and the absorption coefficient (α) of the basalt samples have been determined with Eq. (1).

$$\varepsilon'(\omega) = \left[\varepsilon'_s + (\varepsilon'_\infty - \varepsilon'_s) \times \frac{1 + (\omega\tau)^{1-\alpha}\sin(1/2)\alpha\pi}{1 + 2(\omega\tau)^{1-\alpha}\sin(1/2)\alpha\pi + (\omega\tau)^{2(1-\alpha)}}\right] \quad (1)$$

Here ε'_s and ε'_∞; is dielectric constant in low and high frequencies, respectively. If the absorption coefficient (α) value is zero, the material shows Debye-type feature. If the absorption coefficient is the range of $0 < \alpha < 1$ the material exhibits non-Debye type feature. As seen in Figure 8, Sample 1 and Sample 2 showed non-Debye-type property. This comes from their structural characteristics. This situation; may be attributed to a large content of magnetic components and non-magnetic component Al_2O_3 ratio is low.

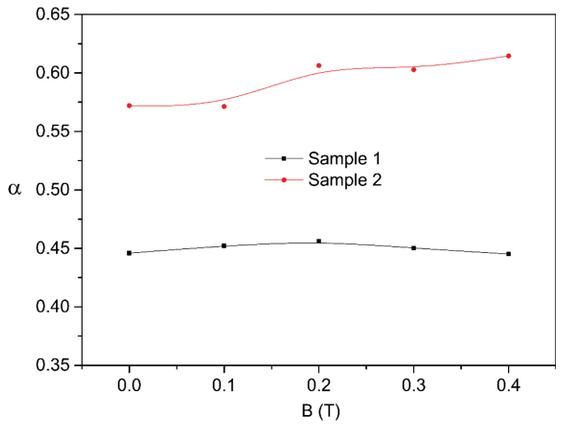


Fig. 8. Changes with the magnetic field of the absorption coefficient of the basalt samples.

In basalt samples, the incident energy must be attenuated, which is a consequence of the equilibrium between electric conductivity and electric losses. As seen in Figure 9, the relaxation time of the basalt samples increases with increasing magnetic field for Sample 1 and Sample 2. In view of magnetic sensor or magnetic absorber, Sample 1 and Sample 2 are believed that allows working in a wide frequency.

To examine the conductivity of the material, it is important to understand their structure. In dielectric spectroscopy, to characterize the electrical properties of materials, usually alternating current (A.C.) conductivity measurements is preferred. Change of angular frequency with a conductivity of basalt samples is given in Figure 10.

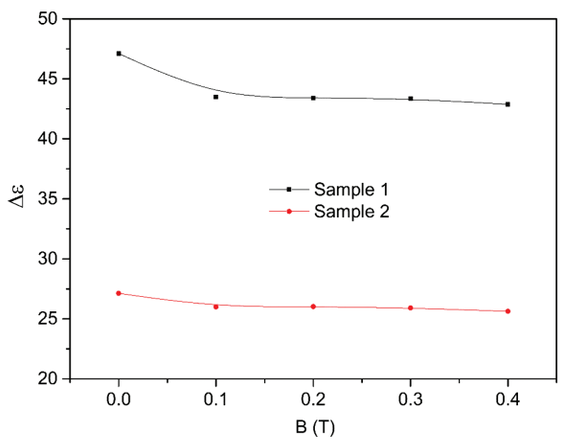


Fig. 7. Changes with the magnetic field of the dielectric strength of the basalt samples.

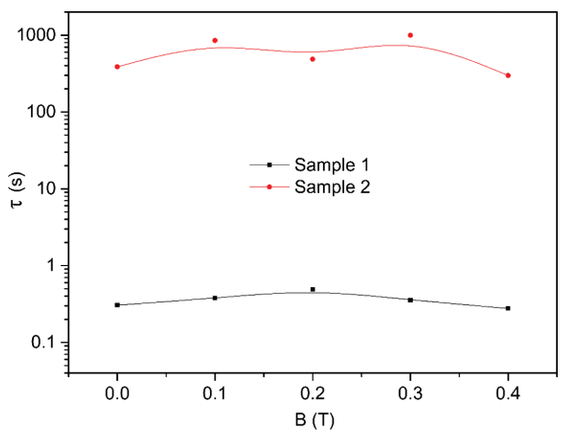


Fig. 9. Changes with the magnetic field of the relaxation time of the basalt samples.

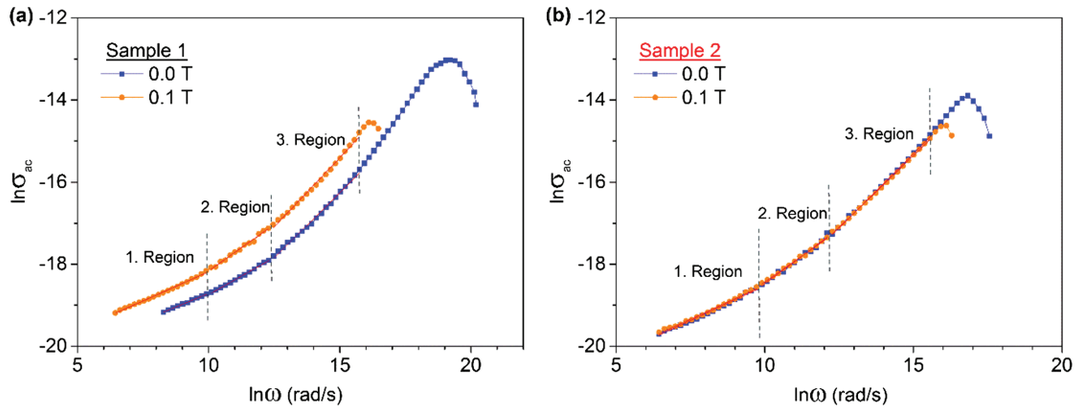


Fig. 10. Change of angular frequency with conductivity of (a) basalt Sample 1 and (b) Sample 2.

With these graphs basalt samples are detected conductivity mechanism. It is used the formula for the conductivity of disordered materials of all kinds depending on the angular frequency;

$$\sigma_{ac} = \sigma(0) + \sigma(\omega) = \sigma_{DC} + A\omega^{s} \tag{2}$$

This formula known as Jonscher's conductivity power law.[17] Here, σ_{AC} is total a.c. conductivity, $\sigma(0)$ is frequency independent conductivity which is D.C. part of conductivity, and $A\omega^{s}$ term is frequency dependent conductivity which is A.C. part of conductivity (σ_{AC}). While $s \approx 0$ state corresponds to D.C. conductivity,[18] $s \approx 0.5$ and $s \leq 0.7 < 1$ conditions represent Correlated Barrier Hoping (CBH) Mechanism[19] and Quantum Mechanical Tunneling (QMT) model,[20] respectively.

"s" parameter is calculated directly with the slope of $\ln \sigma_{ac} = f(\ln \omega)$ function of the samples given in Figure 10. The "s" parameters of the samples given in Table V. The ionic conductivity mechanism of both samples was examined in three regions. The conductivity mechanisms of Sample 1 obey to Correlated Barrier Hoping (CBH) model for all three regions. While, the conductivity mechanism of Sample 2 fits CBH model for region 1 and 2, it obey to Quantum Mechanical Tunneling for region 3.

Table V. "s" parameters of basalt samples.

	s parameter					
	Sample 1			Sample 2		
B (Tesla)	1. Region	2. Region	3. Region	1. Region	2. Region	3. Region
0 T	0.266	0.362	0.637	0.337	0.542	0.725
0.1 T	0.283	0.452	0.674	0.334	0.509	0.700
0.2 T	0.284	0.442	0.675	0.341	0.543	0.749
0.3 T	0.279	0.455	0.677	0.341	0.544	0.756
0.4 T	0.285	0.442	0.675	0.345	0.569	0.754

4. CONCLUSIONS

This study is the first attempt to determine impedance parameters of the relationship between physical and chemical were also identified in volcanic basalt rocks under the magnetic field.

It was found to be a direct correlation between the dielectric strength of the magnetic field. Namely, it is observed that a weakening of the dielectric strength value with the applied magnetic field decreases of Sample 1 having the highest dielectric strength. These results confirm that the magnetic property of basalt is associated with particle clusters which possess a certain magnetic behavior. The magnetic measurements show that basaltic samples are ordered ferromagnetic structure in the particle size form. The iron-rich basalt that makes it featured a ferromagnetic material.

We believe that the basalt rocks may be appraised by this study since the samples have a great absorption rate for low frequency range such as microwaves and radio. Also, we think that the determination of the basalt rocks with high imaginary dielectric component will become more important in future since the energy loss of the rocks is an important quantity for absorption ability.

As a result, the magnetic field caused a decrease in the dielectric strength. Having a minimum dielectric strength of Sample 1 may be attributed to the fact that it has the highest iron content in it. We expect to be able to find application in the industry can provide magnetic shielding, especially in order to usage as aggregate into the wall plaster used with cement or concrete in magnetic resonance and ultrasound room of hospitals.

References and Notes

1. M. Anda, J. Shamshuddin, and C. I. Fauziah. *Catena.* 124, 147 **(2015)**.
2. G. Gillman, D. Burkett, and R. Coventry, *Appl. Geochemistry* 17, 987 **(2002)**.
3. K. Horai, *J. Geophys. Res.* 76, 1278 **(1971)**.

4. A. W. A. El-Shennawi, M. A. Mandour, M. M. Morsi, and S. A. M. Abdel-Hameed, *J. Am. Ceram. Soc.* 82, 1181 **(1999)**.
5. W. A. Deer, R. A. Howie, and J. Zussman (eds.), Introduction to the Rock-Forming Minerals, Mineralogical Society, London **(2013)**.
6. Y. Karabul, L. Amon Susam, O. İçelli, and Ö. Eyecioğlu, *Nucl. Instruments Methods Phys. Res. Sect. A Accel. Spectrometers, Detect. Assoc. Equip.* 797, 29 **(2015)**.
7. A. Çetin, M. Okutan, O. Içelli, Z. Yalçin, S. E. San, R. Kibar, and E. Pesen, *Vacuum* 97, 75 **(2013)**.
8. V. A. Lebedev, E. V. Sharkov, M. Keskin, and V. Oyan, *Dokl. Earth Sci.* 435, 1548 **(2010)**.
9. M. Tapan, *Eur. J. Environ. Civ. Eng.* 19, 94 **(2014)**.
10. P. Gu, P. Xie, Y. Fu, and J. J. Beaudoin, *Cem. Concr. Res.* 24, 86 **(1994)**.
11. W. J. McCarter and R. Brousseau, *Cem. Concr. Res.* 20, 891 **(1990)**.
12. M. Okutan, H. B. Kavanoz, O. Içelli, Z. Yalçin, F. Ay, D. Delipinar, and F. Yakuphanoğlu, *Vacuum* 101, 298 **(2014)**.
13. E. Mattei, S. E. Lauro, G. Vannaroni, B. Cosciotti, F. Bella, and E. Pettinelli, *Icarus* 229, 428 **(2014)**.
14. M. E. Ramia and C. A. Martín, *Appl. Phys. A* 118, 769 **(2015)**.
15. N. Al-Senany, A. A. Al-Ghamdi, E. Al-Hazmi, F. Alnowaiser, M. Ilhan, F. El-Tantawy, and F. Yakuphanoğlu, *J. Nanoelectron. Optoelectron.* 9, 685 **(2014)**.
16. H. Aydin, *J. Nanoelectron. Optoelectron.* 9, 608 **(2014)**.
17. A. K. Jonscher (ed.), Dielectric Relaxation in Solids, Chelsea Dielectrics Press, London **(1983)**.
18. T. Tiwari, N. Srivastava, and P. C. Srivastava, *Int. J. Electrochem.* 2013, 1 **(2013)**.
19. S. R. Elliott, *Adv. Phys.* 36, 135 **(1987)**.
20. A. Ghosh, *Phys. Rev. B* 41, 1479 **(1990)**.